Hydrogen Production by Steam Reforming of Vegetable Oils Using Nickel-Based Catalysts

Maximiliano Marquevich, Xavier Farriol, Francisco Medina, and Daniel Montané*

Department of Chemical Engineering, Rovira i Virgili University, Av. Països Catalans, 26 43007 Tarragona (Catalunya), Spain

Vegetable oils and fats are a renewable resource derived from biomass that can contribute to reduce the net emission of CO_2 into the atmosphere if used to produce hydrogen for fuel-cell-based energy systems. In this paper, we present the results of the steam reforming of several vegetable oils with three different nickel-based commercial catalysts (ICI 46-1, ICI 46-4, and UCI G90C) and two research catalysts (UdeS and HT). The experiments were performed in an isothermal fixed-bed tubular reactor at steam-to-carbon (*S*/*C*) ratios of 9, 6, and 3 and temperatures between 500 and 630 °C. High space velocities of 0.76−1.90 $mol_{carbon}/(g_{cat}\ h)$ were used so that conversions of the feed would be incomplete. Hydrogen productions were from 0.3 to 7.5 $mol_{H_2}/(g_{Ni}\ h)$ depending on the operating conditions. The HT catalyst, which was prepared from a hydrotalcite-like precursor, seems promising for steam reforming vegetable oils because of its very high activity per gram of catalyst. Results for the steam reforming of sunflower, rapeseed, corn, and soybean oils at the same catalyst temperature and *S*/*C* ratio show that oil conversion to gases and hydrogen yields do not depend on the type of vegetable oil. This indicates that the process might be suitable for producing hydrogen from residual oils and fats from food processing, for which process economics are more favorable.

Introduction

Using hydrogen as a fuel and energy carrier is one way of creating an energy system that has a smaller impact on the environment, especially in terms of the emission of gases linked to the greenhouse effect.[1,2] One problem with this hypothetical hydrogen-based energy system is the fact that the technology involved in the production of hydrogen today has a strong effect on the environment. Most hydrogen is produced on an industrial scale from natural gas, LPG, and naphtha by catalytic steam reforming or from heavy oil fractions by partial oxidation.[3] Consequently, hydrogen production, because it is based on fossil fuels, is a net contributor to carbon dioxide emissions and the greenhouse effect. Unless hydrocarbon-based technology is upgraded to incorporate effective methods of carbon sequestration,[4] other options are needed. One alternative is to use renewable resources to produce hydrogen,[5] particularly via the thermal conversion of biomass[6] either by gasification[7−10] or by steam reforming of biomass-derived liquids.[11] Several biomass-derived liquids have been studied: bio-oil from flash pyrolysis of lignocellulosics;[6,12−16] hemicellulose solutions from biomass fractionation;[17] ethanol;[18−20] and vegetable oils and fats, which are an attractive feedstock for hydrogen production because of their low oxygen content and their potentially high yield of hydrogen.[21] Concerning the use of vegetable oils in nonfood applications, rapeseed, canola, and sunflower oils are actually being used in Europe as a fuel in the transportation sector (biodiesel),[22−26] and they have also been studied for the synthesis of biodegradable lubricants[27,28] and for the production of olefins and other hydrocarbons by pyrolysis[29,30] and catalytic cracking.[31] In general, process economics are not favorable for the use of food-grade vegetable oils in energy applications because of their high market value, unless subsidies or tax exemptions are implemented as is done for biodiesel in the European Union. Nevertheless, good economic potential does exist for producing hydrogen from waste oils and fats from the food-processing industry (trap grease).[32]

In a previous paper,[21] we demonstrated that sunflower oil could be satisfactorily converted into hydrogen by steam reforming using a commercial nickel-based catalyst. Hydrogen yields were between 72 and 87% of stoichiometric in experiments at complete oil conversion depending on the steam-to-carbon ratio and temperature of the catalyst, and further conversion of carbon monoxide in a downstream shift reactor could produce hydrogen yields close to the maximum stoichiometric potential. In this paper, we conduct a systematic study at partial conversion of the oil using several industrial and research catalysts. The experiments were conducted in an almost isothermal fixed-bed reactor to obtain data for modeling the reaction kinetics. We selected sunflower oil as the prototype vegetable oil for the study, and some experiments were performed for rapeseed oil, corn oil, and soybean oil under the same reaction conditions to show that the process can be used with other vegetable oils with equivalent results.

Experimental Section

Vegetable Oils. We used four commercial vegetable oils: sunflower oil, rapeseed oil, soybean oil, and corn oil. The elemental compositions (C, H, and O) of the oils were determined with a Carlo Erba EA1108 analyzer and are shown in Table 1 with the calculated C_{18} formulas. The typical composition of the main fatty acids is also included for each oil.[33]

* Author to whom correspondence should be addressed. E-mail: Daniel.Montane@etseq.urv.es. Phone: +(34) 977 559 652. Fax: +(34) 977 559 621.

10.1021/ie010135t CCC: $20.00
Published on Web 10/09/2001

Table 1. CHO Composition of the Vegetable Oils Used in This Study and Their Main Fatty Acids[a]

vegetable oil	sunflower	rapeseed	soybean	corn
		elemental composition (wt %)		
carbon	75.9 ± 0.3	76.3 ± 0.2	76.4 ± 0.2	76.0 ± 0.1
hydrogen	12.1 ± 0.2	12.3 ± 0.1	12.3 ± 0.1	12.1 ± 0.1
oxygen	12.0 ± 0.4	11.3 ± 0.1	11.3 ± 0.3	11.8 ± 0.2
C_{18} formula	$C_{18}H_{34.4}O_{2.1}$	$C_{18}H_{34.9}O_{2.0}$	$C_{18}H_{34.8}O_{2.0}$	$C_{18}H_{34.5}O_{2.1}$
		main fatty acids[33]		
palmitic (16:0)	6.1	3.5	11.7	11.7
estearic (18:0)	3.3	0.9	3.2	1.9
oleic (18:1)	16.9	64.4	23.3	25.2
linoleic (18:2)	73.7	22.3	55.5	60.6
linolenic (18:3)	0.0	8.2	6.3	0.5

[a] According to ref 33.

Table 2. Summary of the Main Properties of the Commercial Steam-Reforming Catalysts

manufacturer and catalyst	shape, size,[a] and surface area (m^2/g)	active agents and carrier support	bulk density compacted (g/cm^3)[b]	application (feedstock)
		United Catalysts Inc. (UCI)		
G90C	Rasching ring, 17 × 7 × 7, SA = 3−15	15% Ni on a ceramic carrier (70−76% Al_2O_3, 5−8% CaO)	0.96 [1.97]	difficult service (low *S*/*C* ratios, $C_3 + C_4$ hydrocarbons, etc.)
		ICI Katalco[c]		
46-1	ring, 17 × 7 × 17, SA = na	10−25% NiO on a refractory carrier, 1.5% K_2O promoted	1.15 [2.52]	high-MW naphtha (bp up to 235 °C, containing up to 25% aromatics)
46-4	ring, 17 × 7 × 17, SA = na	10−25% NiO on a refractory carrier, ZrO_2 promoted	0.99 [2.38]	for use with 46-1

[a] Size specifications are in the format o.d. × i.d × length in millimeters. na = not available. [b] Values in square brackets exclude void fractions. [c] ICI = Imperial Chemical Industries.

Table 3. Composition of the Research Catalysts

catalyst	composition (wt %)
UdeS	15% Ni 10% MgO 5% Cr 65% Al_2O_3 5% La_2O_3
HT	58.6% Ni 13.5% Al 27.9% O

Catalysts. We used several commercial and research nickel-based catalysts specially designed for steam reforming. The characteristics of the commercial catalysts are shown in Table 2. The compositions of the research catalysts, UdeS and HT, are shown in Table 3. The UdeS catalyst was patented and provided by the University of Sherbrooke (Canada),[34] and it was developed for the steam reforming of paraffinic and polycyclic aromatic hydrocarbons. The HT catalyst was prepared in our laboratory[35] from a coprecipitated hydrotalcite-like precursor with a Ni^{2+}/Al^{3+} atomic ratio of 2. Hydrotalcite-like compounds are described by the empirical formula in eq 1, where M^{2+} and M^{3+} are metal cations, A^{x-} represents the *x*-valent anion needed to compensate the net positive charge, *x* is the charge of the anion, *y* is the number of interlayer water molecules, and the ratio $m/(m + n)$ can vary from 0.17 to 0.33 depending on the particular combination of di- and trivalent elements. Supported metal catalysts suitable for hydrogenation and steam reforming are obtained from these precursors by calcination, which yields an oxide of the type $M^{2+}M^{3+}(O)$, and reduction.[35−38]

$$[(M^{2+})_n(M^{3+})_m(OH)_{2(n+m)}]^{m+}[(A^{x-})_{m/x}.yH_2O] \quad (1)$$

The fresh catalysts were crushed into smaller particles ($0.2\ mm < d_p < 0.3\ mm$) and reduced at 600 °C overnight under a constant flow of 0.8 NL/min of an equimolar mixture of hydrogen and nitrogen. Samples of reduced catalysts were characterized by BET and metal surface areas and by X-ray diffraction. BET surface areas were calculated from the nitrogen adsorption isotherms at 77 K in a Micromeritics ASAP 2000 surface analyzer with a value of 0.164 nm^2 for the cross section of the nitrogen molecule. Hydrogen chemisorption was measured by pulses with a Micromeritics Autochem 2910 instrument equipped with a TCD detector. Samples were previously reduced under the same conditions as for the preparation of the catalysts. After reduction, the hydrogen was removed with a flow of 15 cm^3/min of Ar for 30 min at 623 K. The sample was subsequently cooled to room temperature under the same Ar stream, and H_2 pulses (0.047 cm^3) were injected until the eluted area of consecutive pulses was constant. Powder X-ray diffraction (XRD) patterns of the fresh and used catalysts were obtained with a Siemens D5000 diffractometer via nickel-filtered Cu Kα radiation. The patterns were recorded over a range of 2θ angles from 5° to 85° and compared to the X-ray powder references to confirm phase identities. X-ray line-broadening calculations of particle size for the reduced phases were performed by applying the Scherrer equation to the most intense diffraction lines.

Equipment and Experimental Procedure. This study was carried out in the fixed-bed catalytic microreactor schematized in Figure 1. It was constructed with a 12.7-mm ($^1/_2$-in.) o.d. 316L stainless steel tube placed inside an electric furnace with a heating section of 28 cm length. The catalyst was held on a metallic grid placed inside the reactor tube as shown in Figure 2. The temperature of the catalyst bed was measured with three thermocouples (type K, 0.5 mm o.d.) placed inside a 3.18-mm ($^1/_8$-in.) o.d. 316L stainless steel sheath along

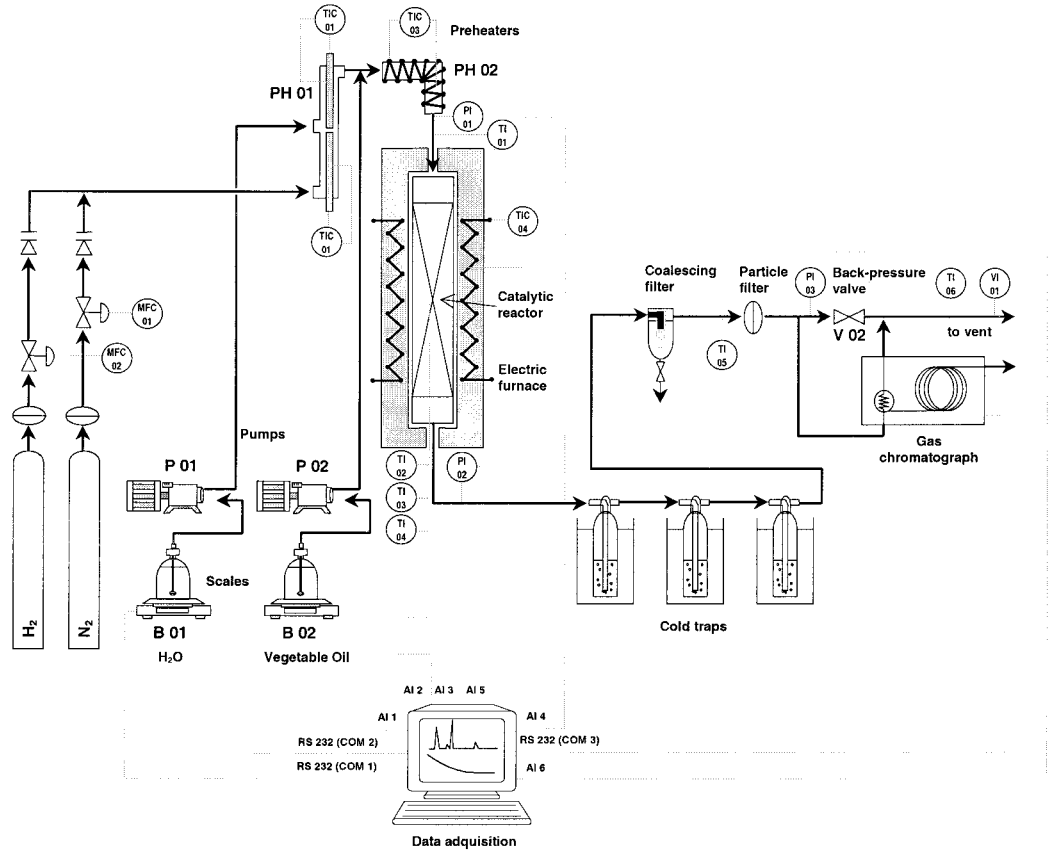

Figure 1. Fixed-bed catalytic reactor unit.

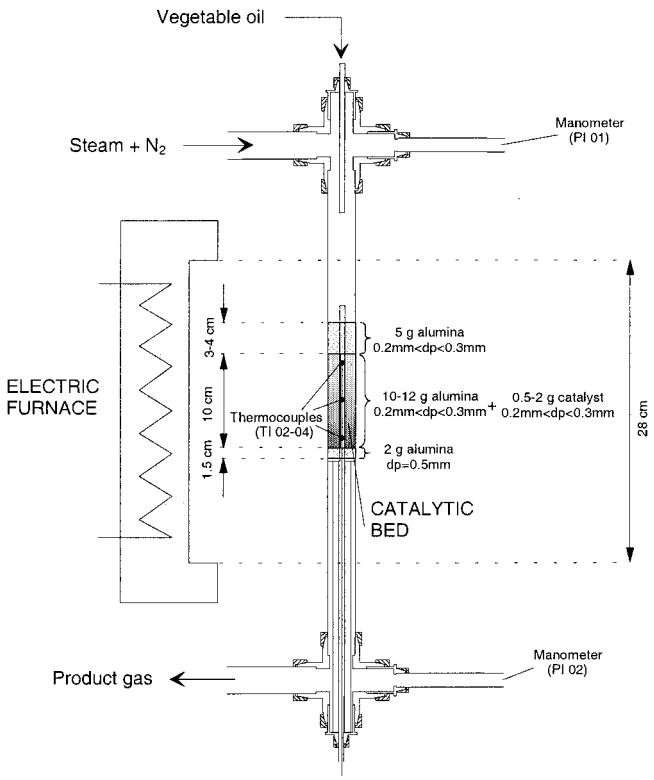

Figure 2. Arrangement of the catalyst inside the reactor tube.

the center of the reactor. The first thermocouple (TI 02) measured the temperature at the beginning of the bed, the second (TI 03) at the half-height of the bed, and the last (TI 04) at the bed outlet. The differences in temperature never exceeded 10−15 °C during an experiment, and the bed was therefore considered to operate isothermally. The average temperature was used as the temperature of the catalyst. Water and vegetable oil were pumped at room temperature by two metering pumps (Pulsatron Series E plus). Water was vaporized in a preheater (PH 01) consisting of two 500-W electric heaters held at 410 °C. Nitrogen was mixed with steam in the preheater and used as the carrier gas and internal standard for gas analysis by GC. A mass flow controller (MFC 01) regulated the flow rate of nitrogen. The vegetable oil was mixed with steam and nitrogen at the entrance to the reactor tube, and a thermocouple (TI 01) and a transducer (PI 01) were placed at the mixing point to measure temperature and pressure at the reactor entrance. Pressure was measured also at the reactor outlet (PI 02) to determine the differential pressure through the catalyst bed. Excess steam and organic condensables were recovered in three cold traps, and the gas was finally treated in a coalescing filter (Headline 710N, 1 μm). A portion of the dry gas passed through the gas chromatograph sample loop, while the rest flowed through a back-pressure regulator (V 02) that controlled the pressure of the system. The volumetric flow rate of dry gas was measured at atmospheric pressure with a turbine-type meter (VI 01), and the temperature of the gas was recorded to calculate the mass flow rate of gas. Water and oil feed rates, temperatures in the bed (TI 02−04), pressures (PI 01−03), and gas flow rate (VI 01) were recorded on a PC-based data acquisition system and continuously monitored.

Product analysis. The composition of the gas was determined by an on-line gas chromatograph (Hewlett-Packard 5890) equipped with a Carboxen 1000 packed column (1.5 m, 3.18-mm ($^1/_8$-in.) o.d., 60/80 mesh) and

Table 4. Operating Conditions of the Tests to Evaluate Mass Transport Limitations

series[a]	catalyst and load (g)	d_p (mm)	temperature (°C) furnace	temperature (°C) average	oil flow rate (g/min)	*S/C* ratio (mol/mol)	N_2 flow rate (L/min)	time on stream (min)
a	ICI 46-1, 2 g	0.2−0.3	650	629	0.4	6	0.27	159
			600	590				102
			550	557				100
b	ICI 46-1, 1 g	0.2−0.3	650	629	0.2	6	0.14	66
			600	589				71
			550	551				64
c	ICI 46-1, 2 g	0.4−0.6	650	624	0.4	6	0.27	63
			600	586				62
			550	540				61

[a] *a*, base case; *b*, external transport; *c*, internal transport.

a thermal conductivity detector. A pneumatic 10-way valve (Valco A-4C10UWT) was used to inject the sample through a 1-mL sample loop, and helium was used as the reference gas. This configuration allows hydrogen, nitrogen, methane, carbon dioxide, carbon monoxide, acetylene, ethylene, ethane, and a C_3 peak (propane and propylene) to be separated simultaneously in an analysis that runs for 20 min. The organic liquid recovered in the condenser was analyzed qualitatively to monitor the extent of cracking by GC-MS using a Hewlett-Packard 5890 chromatograph with a 5989A mass spectrometer system. Its elemental composition was determined with a Carlo Erba EA1108 analyzer and used to calculate the mass balance closure for carbon.

Operating Conditions. A systematic study of the influence of temperature and steam-to-carbon (*S/C*) ratio was performed at constant near-atmospheric pressure. Duplicated experiments were conducted for 1−2 h under steady-state conditions at steam-to-carbon ratios of 3, 6, and 9 and furnace temperatures of 550, 600, and 650 °C, which resulted in catalyst temperatures of between 500 and 630 °C. We used a definition of space velocity based on the moles of carbon present in the reactor feed. The units for the hourly space velocity, denoted M_{C1}HSV, are moles of carbon in the feed per unit mass of catalyst (in grams) per unit time (in hours). We used a space velocity (M_{C1}HSV) of 0.76 $mol_{carbon}/(g_{cat}$ h) for all the experiments, except for those performed with the HT catalyst, where a M_{C1}HSV of 1.90 $mol_{carbon}/(g_{cat}$ h) was used. The space velocity was set by loading a different amount of catalyst into the reactor and keeping all the other variables constant. The amount of catalyst was selected for an appropriate level of oil conversion (approximately 5−80%, depending on the temperature and the *S/C* ratio).

The oil flow rate and the catalyst particle size were selected to minimize, as far as possible, the mass and energy transport limitations. Hence, high flow rates of feed and the smallest particle diameters feasible for our reactor system were used.[39] To verify that there was no significant intraphase (internal) or interphase (external) gradients at the selected conditions, three series of tests were done in which the particle size or the gas velocity was varied at constant space velocity. Each series included experiments at three temperatures (between 550 and 650 °C). The catalyst ICI 46-1 was used for sunflower oil at the experimental conditions shown in Table 4. Series a is the base case for which the catalyst particle size was between 0.2 and 0.3 mm, and the oil flow rate was set at 0.4 g/min. In series b, the gas velocity was decreased by reducing the flows of water, oil, and nitrogen to one-half of those of the base case, with the mass of catalyst also reduced to maintain the same space velocity. In series c, the gas velocity was maintained as in the base case (series a), but the particle size was doubled. Figure 3 shows plots of the carbon conversion to gases (CO, CO_2, and CH_4) against the average temperature of the catalytic bed for each series. There are no significant differences observed between the results of series a and b and the results of series a and c, which shows that external and internal mass transfer limitations can be considered irrelevant under these operating conditions. Energy transport limitations cannot be reliably checked experimentally. To minimize heat transfer limitations in the bed, the catalysts were mixed with tabular α-alumina (Alcoa, T-60, 0.2−0.3 mm) at a weight ratio of 6−10 g of α-alumina per gram of catalyst.

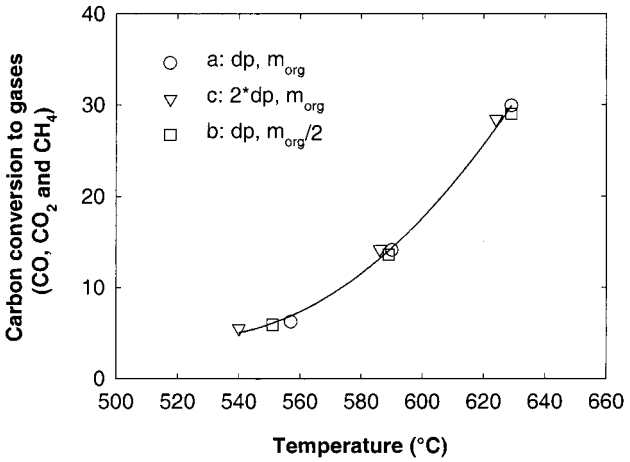

Figure 3. Analysis of the mass transfer limitations to reaction rate. Carbon conversion to gases (CO, CO_2, and CH_4) against average temperature of the catalytic bed at several conditions: d_p = 0.2−0.3 mm, m_{org} = 0.40 mol/min.

Steam reforming is a strongly endothermic reaction process that requires high catalyst temperatures (well over 500 °C) for satisfactory operation. At these temperatures, thermal cracking is a competing and unavoidable process during the steam reforming of vegetable oils. Thermal cracking of vegetable oils starts at 250−350 °C by cleavage of the ester bonds to yield free fatty acid chains. At higher temperatures, fatty acids decompose by decarboxylation and decarbonylation to saturated and unsaturated hydrocarbons. These hydrocarbons are then further converted by ethylene elimination, isomerization, and hydrogen-transfer reactions to yield ethylene, propylene, and other small hydrocarbons. Short-chain oxygenated hydrocarbons are formed by the C−C scission of the unsaturated fatty acid chains, cycloolefins appear as a result of cyclization reactions, and aromatics also originate at high cracking severity.[30] We used tabular α-alumina to dilute the catalyst in the reforming experiments, but α-alumina has some acid

Table 5. Cracking of Sunflower Oil: Experimental Conditions, Flow Rate and Composition of the Product Gas, and Percentage of Carbon (from Feed) Converted to Gas Products (CO, CO_2, CH_4, C_2, and C_3^+)[a]

	temperature (°C)				time on stream	gas flow rate[b]	gas composition[b] (%)							carbon in gases (%
expt	furnace	TI 02	TI 03	TI 04	(min)	(L/min)	CO	CO_2	CH_4	C_2H_2	C_2H_4	C_2H_6	C_3^+	of feed)
100	750	738	740	715	120	0.170	14.6	9.6	13.6	2.5	40.8	4.4	14.5	52.8
109	750	749	749	710	137	0.160	11.6	14.0	12.7	1.6	37.4	4.8	17.9	50.5
105	700	697	696	671	124	0.080	10.6	12.7	12.7	4.5	39.5	5.1	14.9	25.1
101	650	651	649	630	58	0.030	9.5	13.8	10.8	7.6	32.0	9.7	16.6	9.6
108	650	649	649	625	119	0.020	10.6	10.8	18.1	5.9	34.8	7.4	12.4	6.1
106	600	597	594	582	115	0.010	8.8	8.7	20.9	9.8	25.9	9.5	16.3	3.1
102	550	549	548	535	110	0.001	8.2	17.4	38.1	8.1	20.3	7.9	n.d.	0.2

[a] All experiments were conducted at a *S/C* ratio of 6. [b] N_2-free basis.

sites that can favor the formation of coke. Tabular α-alumina was purposely chosen to operate at high temperature because it has a small surface area and few acid sites, but we had to verify that a massive oil cracking on the α-alumina surface did not occur. We therefore conducted a series of tests in the absence of nickel catalyst at different temperatures to establish the extent of cracking of sunflower oil (either thermal or catalyzed by α-alumina) in the system. The tests were carried out using the reactor filled with pure tabular α-alumina to the same length as in the steam-reforming experiments at a steam-to-carbon ratio of 6; furnace temperatures of 550, 600, 650, 700, and 750 °C; and the same oil feed rates as in the steam-reforming experiments.

Results and Discussion

Evaluation of Oil Cracking. The process conditions and the main results of the cracking experiments are shown in Table 5. All tests were conducted at an *S/C* ratio of 6 (flow rates of 0.4 g/min for sunflower oil, 2.74 g/min for steam, and 0.28 NL/min for the carrier gas N_2) and maintained for around 2 h at steady-state conditions. We studied temperatures between 550 and 750 °C, which is a typical range for steam reforming. Experiments 109 and 108 are duplicates of experiments 100 and 101, respectively. The good agreement between the results verifies the reproducibility of the equipment. The results show that the degradation of sunflower oil increased as the temperature was increased. At the highest furnace temperature, 750 °C (expt 100), 52.8% of the carbon in the oil was converted to gas products (CO, CO_2, CH_4, C_2^+), which indicates a high level of cracking. This conversion dropped significantly as the temperature decreased. Below 650 °C (expts 101 and 108), the percentage of carbon found in gas products was less than 10% of the carbon in the feed. From this temperature, the thermal- or catalytic-cracking process increased dramatically. The amount of sunflower oil converted to gases by cracking doubled when the temperature was increased from 650 to 700 °C (expt 105), the gas product flow rate changed from 0.025 to 0.080 L/min and the carbon converted to gases increased from 8 to 25%. Ethylene was always the main cracking product detected in the gas, and its concentration increased as the temperature increased. Qualitative GC-MS analysis of the organic fraction of the condensed liquid product showed similar trends. Figure 4 shows the gas chromatogram of three samples of liquid products, corresponding to experiments 102, 108, and 100, which were performed at 550, 650, and 750 °C, respectively. We can see that the variety of cracking products and the intensities of their peaks increased as the temperature increased. Aromatic products (benzene, methyl and ethyl benzene, etc.) and linear hydrocarbons (mainly olefins) were abundant at 750 °C, but they were not detected at 550 °C. At the intermediate temperature of 650 °C, some of these compounds were detected, but their concentrations were very low. The fatty acids (C_{16} and C_{18}) evolved in the opposite sense, decomposing at the higher temperatures to yield smaller hydrocarbons.

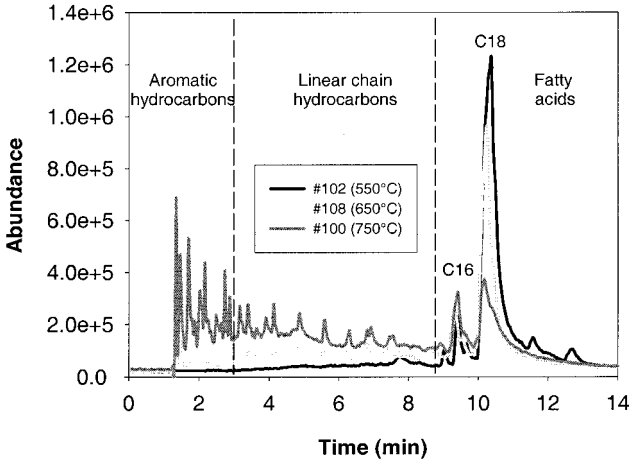

Figure 4. Comparison of the GC analysis of the samples of the organic liquid product condensed at several cracking temperatures. Peaks identified by mass spectra.

From these results, it is clear that cracking will be a competing process during the steam reforming of vegetable oils. Upon heating above 300 °C, the fatty acids will be liberated by cleavage of the ester bonds, a fraction of the fatty acids will decompose, and the cracking products will be steam reformed simultaneously with the remaining fatty acids. The predominant route for the conversion of fatty acids to hydrogen will depend on the relative rates of the processes (i.e., cracking of the fatty acids and steam reforming of the cracking products vs direct reforming of the fatty acids). However, extensive cracking of the oil yields high concentrations of ethylene and aromatics, which are well-known precursors for catalyst deactivation by coke deposition.[21,40,41] Consequently, we selected a temperature range of 500−650 °C to study the steam reforming of vegetable oils in order to limit the extent of the cracking reactions and the possibility of catalyst coking.

Steam Reforming of Sunflower Oil. The operating conditions for each experiment, test number, type and load of the catalyst, *S/C* ratio, furnace temperature, average temperature of the bed, reactor pressure, and duration of the experiment are shown in Table 6. In all experiments, the carrier gas (N_2) flow rate was 0.26−0.29 NL/min. The *S/C* ratios studied (9, 6, and 3) were obtained by setting the steam flow rate to 4.10, 2.74, and 1.37 g/min, respectively, and keeping the flow rate

Table 6. Steam Reforming of Sunflower Oil Using Commercial and Research Catalysts: Operating Conditions[a]

run	catalyst	catalyst load (g)	*S*/*C* ratio (mol/mol)	temperature (°C) furnace	temperature (°C) average	reactor pressure (bar)	time on stream (min)
			(A) Commercial Catalysts				
136	UCI G90C	2.0	6	650	622	1.33	108
137				600	584	1.28	100
138				550	541	1.20	104
140				525	518	1.23	60
172	ICI 46-1	2.0	9	650	629	1.37	59
168				650	617	1.69	100
169				600	573	1.63	100
170				550	528	1.54	39
115			6	650	624	1.27	95
184				600	583	0.59	63
118				550	557	1.09	100
185				550	540	0.53	62
148			3	650	624	1.21	110
149				600	588	1.16	101
150				550	550	1.02	105
142	ICI 46-4	2.0	6	650	622	1.20	107
143				600	581	1.18	108
144				550	540	1.10	97
147				530	523	1.04	61
			(B) Research Catalysts				
173	UdeS	2.0	9	650	607	1.97	101
174				600	568	1.81	100
175				550	529	1.79	101
126			6	650	618	1.59	60
123				650	614	1.51	101
124				600	580	1.46	99
125				550	541	1.37	102
127				500	496	1.27	60
154			3	650	603	1.09	111
155				600	572	1.00	101
158				600	572	1.01	60
156				550	533	0.85	99
217	HT	0.8	9	650	587	2.22	60
180				600	553	1.49	100
218				600	552	2.11	60
181				550	516	1.39	100
219				550	515	1.95	60
214			6	650	589	1.67	60
215				600	556	1.60	60
216				550	524	1.47	60
220			3	650	606	1.22	60
221				600	571	1.04	60
222				550	535	0.82	60

[a] All experiments were conducted at a sunflower oil flow rate of 0.4 g/min and a carrier gas flow rate of 0.26−0.29 L/min.

of vegetable oil constant at 0.40 g/min. The research catalysts and the ICI 46-1 catalyst were studied at all three steam-to-carbon ratios, whereas the ICI 46-4 and the UCI G90C catalysts were studied only at the *S*/*C* ratio of 6. The most relevant results for the steam reforming of sunflower oil are given in Table 7. This table shows the gas flow rate, gas composition (on a N_2-free basis), and percentage of carbon (from the feed) that was converted to gas products. The production of hydrogen, expressed in moles of H_2 per unit mass of nickel in the catalyst (in grams) per unit time (in hours), was selected to measure the activity of the catalysts. Figures 5−7 show plots of the production of H_2 against the average temperature of the bed for each catalyst and for *S*/*C* ratios of 9, 6 and 3, respectively. Generally, the production of H_2 varied between 0.3 and 7.5 $mol_{H_2}/(g_{Ni}$ h), mainly depending on the catalyst and the operating conditions. The gas product flow rate was between 0.03 and 1.56 L/min, and the percentage of carbon converted to gases (CO, CO_2, and CH_4) was between 1.7 and 78.9%.

Effect of Temperature. Carbon conversion to gases and hydrogen production grew as the reaction temperature was increased for all catalysts and *S*/*C* ratios tested. Figures 5−7 show that this trend is almost linear in the range of working temperatures. C_2 and C_3^+ compounds, which are cracking products, were found in very small amounts in the product gas. The percentage of carbon (from the feed) that was recovered as C_2 and C_3^+ products was never more than 6.7% (expt 115), and for the vast majority of the experiments, it was less than 2%. These values are lower than those obtained in the cracking experiments performed with the α-alumina bed, which indicates that cracking products were also converted by the reforming catalysts. However, only the HT catalyst reached a high conversion of cracking products. For example, at an *S*/*C* ratio of 6 and a temperature of 650 °C, the fraction of carbon converted to C_2 and C_3^+ gases was 6.3% for the cracking experiment, 4.0−6.0% for the commercial catalysts and the UdeS catalyst, and only 0.9% for the HT catalyst.

Effect of S/C Ratio. Data in Figures 5−7 show that the effects of the *S*/*C* ratio on the production of hydrogen were similar for the ICI 46-1 and UdeS catalysts, whereas the HT catalyst presented a different behavior. For the ICI 46-1 and UdeS catalysts, the production of

Table 7. Steam Reforming of Sunflower Oil Using Commercial and Research Catalysts: Experimental Results

expt	catalyst	gas flow rate[a] (L/min)	gas composition (%)								carbon in gases (% of feed)	
			H_2	CO	CO_2	CH_4	C_2H_2	C_2H_4	C_2H_6	C_3^+	(CO, CO_2, CH_4)	(C_2, C_3^+)
						(A) Commercial Catalysts						
136	UCI G90C	0.86	69.5	5.2	23.5	0.7	0.2	0.6	0.3	0.3	39.9	4.3
137		0.41	70.0	4.2	24.2	0.5	0.2	0.6	0.3	0.3	20.2	2.1
138		0.18	71.0	2.9	24.6	0.4	0.2	0.6	0.3	0.3	8.8	1.0
140		0.09	72.5	2.7	23.1	0.4	0.2	0.7	0.3	0.2	4.4	0.5
172	ICI 46-1	0.60	68.5	4.7	23.5	0.9	0.3	1.8	0.5	0.6	30.1	6.0
168		0.31	66.4	5.1	23.6	1.3	0.4	2.6	0.7	1.0	21.3	6.3
169		0.11	69.7	3.2	22.3	1.1	0.5	2.6	0.7	0.9	5.8	2.3
170		0.03	70.5	1.4	24.8	0.7	0.3	1.6	0.5	0.2	1.7	0.5
115		0.84	69.1	4.5	23.7	0.8	0.3	1.3	0.4	0.4	37.4	6.7
184		0.35	69.7	2.7	25.7	0.5	0.2	0.9	0.3	0.4	16.2	2.2
118		0.14	70.0	3.0	24.0	0.7	0.3	1.6	0.5	0.6	6.2	1.5
185		0.13	70.8	1.9	25.6	0.4	0.2	0.8	0.3	0.3	6.5	0.8
148		1.07	68.1	7.6	22.1	1.0	0.3	0.4	0.5	0.2	53.7	5.2
149		0.56	69.6	3.7	24.9	0.7	0.3	0.4	0.4	0.3	28.5	2.9
150		0.25	69.8	1.8	26.6	0.5	0.3	0.6	0.4	0.3	11.8	1.4
142	ICI46-4	0.89	68.9	6.2	22.9	0.8	0.2	0.7	0.4	0.3	44.8	4.6
143		0.58	70.7	3.0	25.2	0.4	0.1	0.3	0.2	0.1	29.3	1.6
144		0.25	71.0	1.8	26.1	0.3	0.1	0.4	0.2	0.0	11.6	0.6
147		0.15	71.7	1.5	25.8	0.3	0.1	0.5	0.2	0.0	7.0	0.4
						(B) Research Catalysts						
173	UdeS	0.80	66.4	9.6	20.8	1.1	0.3	1.2	0.5	0.6	38.8	4.9
174		0.39	68.9	4.2	25.1	0.5	0.2	0.7	0.4	0.4	17.9	2.1
175		0.14	69.0	3.5	25.4	0.6	0.3	0.8	0.5	0.5	6.6	0.9
126		1.15	70.0	6.4	22.5	0.7	0.1	0.2	0.2	0.0	58.4	2.0
123		1.09	68.4	9.2	20.6	0.8	0.2	0.4	0.4	0.2	53.2	2.7
124		0.67	70.5	3.7	24.7	0.5	0.2	0.2	0.2	0.0	30.8	1.3
125		0.30	70.3	2.3	26.1	0.4	0.2	0.3	0.3	0.1	13.7	0.8
127		0.08	47.3	3.1	46.6	0.9	0.4	1.0	0.7	0.6	4.4	0.6
154		1.34	67.5	10.4	20.2	1.2	0.2	0.2	0.3	0.1	66.6	1.9
155		0.90	69.6	5.1	24.1	0.9	0.1	0.1	0.2	0.0	41.8	1.0
158		0.88	69.4	5.3	23.9	1.0	0.1	0.1	0.2	0.0	41.4	1.2
156		0.42	70.5	2.1	26.6	0.4	0.1	0.1	0.2	0.0	18.9	0.5
217	HT	1.46	69.5	4.2	24.3	1.7	0.0	0.1	0.0	0.0	70.8	0.9
180		0.93	71.7	2.0	25.7	0.4	0.0	0.1	0.1	0.0	40.8	0.7
218		0.91	71.3	1.9	26.0	0.6	0.0	0.1	0.0	0.0	41.3	0.5
181		0.46	72.1	0.8	26.8	0.1	0.0	0.1	0.1	0.0	19.7	0.3
219		0.50	71.8	0.7	27.1	0.2	0.0	0.1	0.0	0.0	21.7	0.3
214		1.56	67.5	6.4	23.1	2.8	0.0	0.1	0.0	0.0	78.9	0.8
215		1.05	69.5	3.4	25.1	1.8	0.0	0.1	0.1	0.0	50.0	0.9
216		0.60	71.3	1.4	26.7	0.4	0.0	0.1	0.0	0.0	26.7	0.3
220		1.42	66.6	9.0	21.1	3.0	0.0	0.2	0.1	0.0	72.0	1.4
221		0.94	68.9	4.6	24.2	1.7	0.3	0.2	0.1	0.0	43.5	2.0
222		0.51	70.8	2.0	26.2	0.7	0.1	0.2	0.1	0.0	22.7	0.5

[a] N_2-free basis.

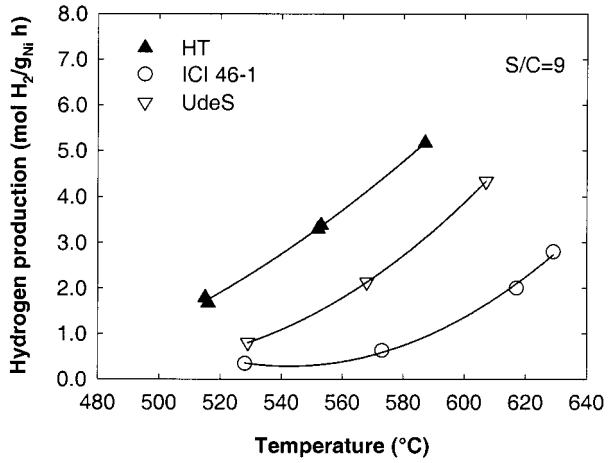

Figure 5. Hydrogen production (in moles of H_2 produced per gram of nickel per hour) against average temperature of the catalytic bed for an *S*/*C* ratio of 9. Lines only indicate trends.

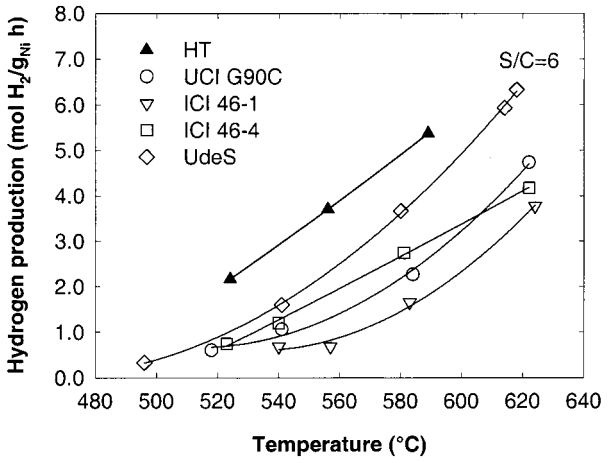

Figure 6. Hydrogen production (in moles of H_2 produced per gram of nickel per hour) against average temperature of the catalytic bed for an *S*/*C* ratio of 6. Lines only indicate trends.

hydrogen per gram of nickel in the catalyst grew when the *S*/*C* ratio was lowered from 9 to 3. For the HT catalyst, the production of hydrogen was almost the same for the *S*/*C* ratios of 9 and 6 for all of the temperatures studied, whereas it decreased significantly when the *S*/*C* ratio was lowered to 3. At an *S*/*C* ratio of

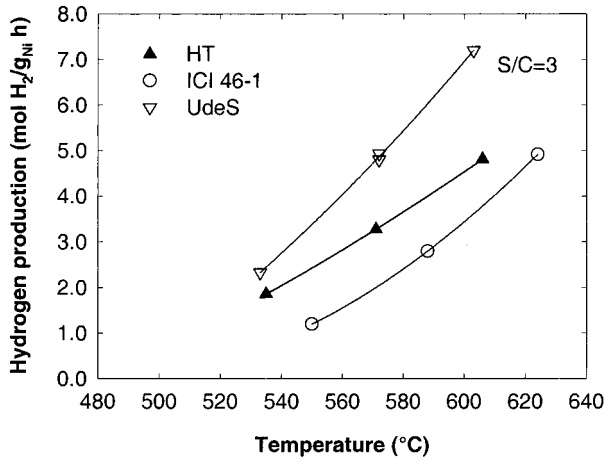

Figure 7. Hydrogen production (in moles of H_2 produced per gram of nickel per hour) against average temperature of the catalytic bed for an *S/C* ratio of 3. Lines only indicate trends.

Table 8. Results of the Catalyst Characterization

catalyst	BET area (m^2/g)	metal area (m^2/g)	XRD phases detected[a] B	A
UCI G90C	6.1	0.2	Ni (45.7)	Ni (57.5), NiO
ICI 46-1	12.2	0.4	Ni (15.2)	Ni (28.7), NiO
ICI 46-4	12.6	0.5	Ni (6.5)	Ni (12.5), NiO
UdeS	99.9	1.7	Ni (5.5), NiO	Ni (16.7), NiO
HT	104.0	17.2	Ni (6.7)	Ni (23.0), NiO

[a] B, before reaction; A, after reaction. In parentheses are the nickel particle sizes (in nanometers).

9 (Figure 5), the HT catalyst was around 10 times more active than the ICI 46-1 in the range of temperatures studied and had nearly double the activity of the UdeS catalyst. At an *S/C* ratio of 6, the HT catalyst had double the activity of the commercial catalysts and was also slightly more active than the UdeS catalyst. However, at an *S/C* ratio of 3, UdeS was the more active catalyst, but the activity of the HT was still higher than that of the ICI 46-1. The dissimilar behavior of the activity of the catalysts with the *S/C* ratio is related to their different characteristics.

Effect of Catalyst. Conversion was always higher for the HT catalyst, although the amount loaded into the reactor (0.8 g) was lower than that loaded for the other catalysts (2.0 g). For example, at a reaction temperature of 580−590 °C and an *S/C* ratio of 6, the conversion of carbon into gas products (CO, CO_2, and CH_4) was 78.9% for the HT catalyst, but 20.2, 16.2, 29.3, and 30.8% for UCI G90, ICI 46-1, ICI 46-4, and UdeS, respectively. Table 8 shows the main properties of the catalysts. The BET surface area was 6.1 m^2/g for UCI G90C, 12.2 m^2/g for ICI 46-1, and 12.6 m^2/g for ICI 46-4, whereas it was about 100 m^2/g for UdeS and HT. Table 8 also shows the metal areas calculated by hydrogen chemisorption. The HT catalyst had the highest metal area (17.2 m^2/g), followed by UdeS (1.7 m^2/g), and the commercial catalysts had areas below 0.5 m^2/g. The nickel particulate sizes are also presented in Table 8. They were 6.7 nm for the HT catalyst, 5.5 nm for UdeS, 6.5 for ICI 46-4, 15.2 for ICI 46-1, and 45.7 for UCI G90C. Figure 8 shows the X-ray diffraction spectra of all of the catalysts before the reaction, and Figure 9 shows the spectra obtained for the used catalysts. Before the reaction, only the Ni phase was detected for the HT catalyst, but for the other catalysts, the NiO phase and other not as well characterized phases were detected. After the reaction, there was a greater abundance of

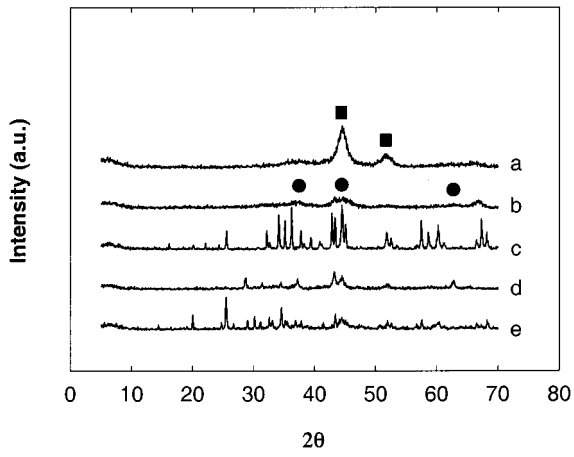

Figure 8. X-ray diffraction spectra of the catalysts before reaction. (a) HT, (b) UdeS, (c) UCI G90C, (d) ICI 46-1, and (e) ICI 46-4. Main phases detected: ■, Ni; ●, NiO.

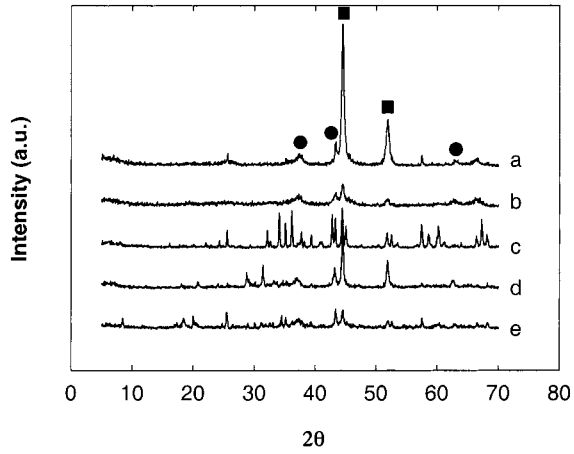

Figure 9. X-ray diffraction spectra of the catalysts after reaction. (a) HT, (b) UdeS, (c) UCI G90C, (d) ICI 46-1, and (e) ICI 46-4. Main phases detected: ■, Ni; ●, NiO.

Table 9. Steam Reforming of Vegetable Oils: Experimental Conditions[a]

run	vegetable oil	average temperature (°C)	reactor pressure (bar)	time on stream (min)
210	sunflower	570	1.50	120
211	rapeseed	572	1.49	120
212	corn	575	1.51	121
213	soybean	579	1.52	120

[a] All experiments were performed using a 2-g load of catalyst ICI 46-1, an organic flow rate of 0.40 g/min, and an *S/C* ratio of 6.

the NiO phase for all catalysts. We also observed an increase in the nickel particle sizes as a result of sintering, which was probably caused by steam and the metal phase interacting at high temperatures. Sintering was more important for the catalysts whose metal particles were smaller.

The differences in BET and metal areas explain the superior activity of the HT catalyst and its different behavior with the variation of the *S/C* ratio. It is commonly accepted that, during steam reforming, water adsorbs preferentially on the catalyst support, which has to be formulated to allow mobility for water molecules adsorbed on the surface. Simultaneously, the organic molecules adsorb preferentially on the metal surface (Ni), and the steam-reforming reaction takes place at the metal−support interface. Hence, three

Table 10. Steam Reforming of Vegetable Oils: Results

run	gas flow rate[a] (L/min)	gas composition[a] (%)								hydrogen production [$mol_{H_2}/(g_{cat}\ h)$]	carbon in gases (% of feed)	
		H_2	CO	CO_2	CH_4	C_2H_2	C_2H_4	C_2H_6	C_3^+		(CO, CO_2, CH_4)	(C_2, C_3^+)
210	0.615	69.4	4.6	24.7	0.6	0.2	0.3	0.2	0.1	0.51	27.9	1.5
211	0.605	70.0	4.2	24.6	0.5	0.2	0.3	0.3	0.2	0.50	27.2	1.8
212	0.610	70.1	4.3	24.5	0.5	0.2	0.3	0.2	0.2	0.50	27.2	1.8
213	0.607	69.5	4.5	24.6	0.5	0.2	0.4	0.3	0.2	0.50	28.0	2.2

[a] N_2-free basis.

factors related to the catalyst structure influence the activity of a steam reforming catalyst: the metal area, the metal particle size, and the support (BET) area and ability to adsorb water. Both the G90C and the 46-1 catalysts have low BET and metal areas, and when high *S*/*C* ratios are used, this might cause water to compete with the organic species for the metal surface, lowering the observed reaction rate. The UdeS catalyst has a high BET area, indicating a good capacity for water adsorption, but the metal area is low, and water competition for the metallic surface also occurs at high *S*/*C* ratios. For the HT catalyst, the BET area is also large, but the metal area is 10 times the area of the UdeS catalyst and 40 times that of the 46-1 catalyst. Consequently, the competition of water for the metal sites does not become determinant until very high water partial pressures are used (high *S*/*C* ratios).

Steam Reforming of Other Vegetable Oils. We also tested rapeseed oil, corn oil, and soybean oil as feedstock for the process. They were chosen because of their strong potential in renewable energy applications and their abundance on the world market.[42] The steam-reforming experiments for these oils were carried out using 2 g of the ICI 46-1 catalyst diluted with α-alumina at a steam-to-carbon ratio of 6 and a furnace temperature of 600 °C. The flow rates of oil and steam were set at 0.40 and 2.74 g/min, respectively, whereas the flow rate was 0.29 L/min for nitrogen. Each experiment was conducted for 2 h with all variables of the system kept at steady-state conditions. Other relevant parameters are shown in Table 9. Also, an experiment with sunflower oil was performed under the same conditions for comparison. Table 10 shows the flow rate and composition of the gas, the production of hydrogen, and the percentage of carbon (from feed) converted to gas products. We can see that the results for these four vegetable oils were very similar, as all differences were of the same order of magnitude as the experimental error. The rate of hydrogen formation was 0.50−0.51 $mol_{H_2}/(g_{cat}\ h)$ for all the oils, and there were no significant differences among the other variables. This result is logical if we consider that the oils tested have very similar compositions, with oleic and linoleic as the main fatty acids in varying proportions. The main implication of this comparative test is that our conclusions for the steam reforming of sunflower oil can be extended to a complete group of the most important vegetable oils and also to waste fats from the food industry where there is a significant presence of the fatty acids that form the oils tested in this study.[32]

Conclusions

Hydrogen can be produced from vegetable oils by catalytic steam reforming using nickel-based catalysts and at process conditions very similar to those used industrially for the steam reforming of hydrocarbons. Because of their activity, which is nearly 10 times higher than that of commercial steam-reforming catalysts, nickel-based catalysts prepared from hydrotalcite-like precursors are promising materials although extended tests are needed to investigate the performance and deactivation of these catalysts in long-duration experiments. In addition to sunflower oil, other vegetable oils such as rapeseed oil, corn oil, and soybean oil can be used as feedstocks for the process with equivalent yields and rates of hydrogen formation. This suggests that fats other than the refined vegetable oils that we tested might be appropriate for hydrogen production, such as residual fats from food processing industries, which offer good economic potential.

Acknowledgment

The authors are indebted to the Spanish Government (Project QUI980464-CO3) and to CIRIT (Catalan Regional Government, Project 1998SGR00098) for financial support. We thank Dr. Esteban Chornet from the University of Sherbrooke for providing samples of the UdeS catalyst. We also thank Dr. Stefan Czernik from NREL for his valuable comments.

Literature Cited

(1) Quakernaat, J. Hydrogen in a Global Long-Term Perspective. *Int. J. Hydrogen Energy* **1995**, *20*, 485.

(2) Armor, J. N. The Multiple Roles for Catalysis in the Production of H_2. *Appl. Catal. A: Gen.* **1999**, *176*, 159.

(3) Ridler, D. E.; Twigg, M. V. Steam Reforming. In *Catalyst Handbook*; Twigg, M. V., Ed.; Wolfe Publishing Ltd: Cleveland, U.K., 1989.

(4) Gaudernack, B.; Lynum, S. Hydrogen from Natural Gas Without Release of CO_2 to the Atmosphere. *Int. J. Hydrogen Energy* **1998**, *23*, 1087.

(5) *U.S. Hydrogen Program Overview*; Report DOE/GO-10095-088; National Renewable Energy Laboratory: Golden, CO, 1995.

(6) Chornet, E.; Wang, D.; Montané, D.; Czernik, S.; Johnson, D.; Mann, M. Biomass to Hydrogen Via Fast Pyrolysis and Catalytic Steam Reforming. In *Proceedings of the 1995 U.S. DOE Hydrogen Program Review*; Report NREL/CP-430−20036; National Renewable Energy Laboratory: Golden, CO, 1995; Vol. 2, pp 707−730.

(7) Evans, R. J.; Knight, R. A.; Onischak, M.; Babu, S. P. Process Performance and Environmental Assessment of Renugas Process. In *Proceedings of Energy from Biomass and Wastes X.*; Klass D. L., Ed.; Institute of Gas Technology: Chicago, IL, 1988.

(8) Hauserman, W. B. High-Yield Hydrogen Production by Catalytic Gasification of Coal or Biomass. *Int. J. Hydrogen Energy* **1994**, *19*, 413.

(9) García, L.; Salvador, M. L.; Arauzo, J.; Bilbao, R. Catalytic Steam Gasification of Pine Sawdust. Effect of Catalyst Weight/Biomass Flow Rate and Steam/Biomass Ratios on Gas Production and Composition. *Energy Fuels* **1999**, *13*, 851.

(10) Caballero, M. A.; Corella, J.; Aznar, M. P.; Gil, J. Biomass Gasification with Air in Fluidized Bed. Hot Gas Cleanup with Selected Commercial and Full-Size Nickel-Based Catalysts. *Ind. Eng. Chem. Res.* **2000**, *39*, 1143.

(11) Czernik, S.; French, R.; Feik, C.: Chornet, E. Production of Hydrogen from Biomass-Derived Liquids. In *Proceedings of the 2000 U.S. DOE Hydrogen Program Review*; NREL/CP-570-28890;

National Renewable Energy Laboratory: Golden, CO, 2000, Vol. 1, pp 130−140.

(12) Mann, M.; Spath, P.; Kadam, K. Technical and Economic Analyses of Hydrogen Production via Indirectly Heated Gasification and Pyrolysis. In *Proceedings of the 1995 U.S. DOE Hydrogen Program Review*; NREL/CP-430-20036; National Renewable Energy Laboratory: Golden, CO, 1995; Vol. 1, pp 205−236.

(13) Wang, D.; Montané, D.; Chornet, E. Catalytic Steam Reforming of Biomass-Derived Oxygenates: Acetic Acid and Hydroxyacetialdehyde. *Appl. Catal. A: Gen.* **1996**, *143*, 245.

(14) Wang, D.; Czernik, S.; Montané, D.; Mann, M.; Chornet, E. Biomass to Hydrogen Via Fast Pyrolysis and Catalytic Steam Reforming of the Pyrolysis Oil or Its Fractions. *Ind. Eng. Chem. Res.* **1997**, *36*, 1507.

(15) Wang, D.; Czernik, S.; Chornet, E. Production of Hydrogen from Biomass by Catalytic Steam Reforming of Fast Pyrolysis Oils. *Energy Fuels* **1998**, *12*, 19.

(16) Marquevich, M.; Czernik, S.; Chornet, E.; Montané, D. Hydrogen from Biomass: Steam Reforming of Model Compounds of Fast Pyrolysis Oil. *Energy Fuels* **1999**, *13*, 1160.

(17) Czernik, S.; French, R.; Feik, C.; Chornet, E. Production of Hydrogen from Hemicellulose-rich Fractions Generated through Steam Fractionation of Biomass. In *Preprints of the 217th ACS National Meeting, Anaheim, CA, 1999*; American Chemical Society: Washington, D.C., 1999; Vol. 44, pp 240−242.

(18) Caballaro, S.; Freni, S. Ethanol Steam Reforming in a Molten Carbonate Fuell Cell—A Preliminary Kinetic Investigation. *Int. J. Hydrogen Energy* **1996**, *21*, 465.

(19) Freni, S.; Maggio, G.; Caballaro, S. Ethanol Steam Reforming in a Molten Carbonate Fuel Cell—A Thermodynamic Approach. *J. Power Sources* **1996**, *62*, 67.

(20) Mariño, F. J.; Cerrella, E. G.; Duhalde, S.; Jobbagy, M.; Laborde, M. A. Hydrogen from Steam Reforming of Ethanol. Characterization and Performance of Copper−Nickel Supported Catalysts. *Int. J. Hydrogen Energy* **1998**, *23*, 1095.

(21) Marquevich, M.; Coll, R.; Montané, D. Steam Reforming of Sunflower Oil for Hydrogen Production. *Ind. Eng. Chem. Res.* **2000**, *39*, 2140.

(22) Ali, Y.; Hanna, M. A. Alternative Diesel Fuels from Vegetable Oils. *Bioresour. Technol.* **1994**, *50*, 153.

(23) Stumbort, M.; Wong, A.; Hogan, E. Hydroprocessed Vegetable Oils for Diesel Fuel Improvement. *Bioresour. Technol.* **1996**, *56*, 13.

(24) Karaosmanoglu, F.; Cigizoglu K. B.; Tüter, M.; Ertekin, S. Investigation of the Refining Step of Biodiesel Production. *Energy Fuels* **1996**, *10*, 890.

(25) Wenzel, G.; Lammers, P. S. Boiling Properties and Thermal Decomposition of Vegetable Oil Methyl Esters with Regard to Their Fuel Suitability. *J. Agric. Food Chem.* **1997**, *45*, 4748.

(26) Scwab, A. W.; Dykstra, G. J.; Selke, E.; Sorenson, S. C.; Pryde, E. H. Diesel Fuel from Thermal Decomposition of Soybean Oil. *J. Am. Oil Chem. Soc.* **1988**, *65*, 1781.

(27) Legrand, J.; Dürr, K. High-Performing Lubricants Based on Renewable Resources. In *Proceedings of the 10th European Conference on Biomass for Energy and Industry, Würzburg, Germany, 1998*; Kopetz, H., Weber, T., Palz, W., Chartier, P., Ferrero, G. L., Eds.; CARMEN: Rimpar, Germany, 1998; pp 90−92.

(28) de Caro, P.; Claude, S.; Poitrat, E.; Gaouyer, J. P.; Gaset, A. Lubricants Based on Renewable Resources: A Promising Value Chain. In *Proceedings of the 10th European Conference on Biomass for Energy and Industry, Würzburg, Germany, 1998*; Kopetz, H., Weber, T., Palz, W., Chartier, P., Ferrero, G. L., Eds.; CARMEN: Rimpar, Germany, 1998; pp 407−410.

(29) Billaud, F.; Dominguez, V.; Broutin, P.; Busson, C. Production of Hydrocarbons by Pyrolysis of Methyl Esters from Rapeseed Oil. *J. Am. Oil Chem. Soc.* **1995**, *72*, 1149.

(30) Idem, R. O.; Katikaneni, S. P. R.; Bakhshi, N. N. Thermal Cracking of Canola Oil: Reaction Products in the Presence and Absence of Steam. *Energy Fuels* **1996**, *10*, 1150.

(31) Katikaneni, S. P. R.; Adjaye, J. D.; Bakhshi, N. N. Studies on the Catalytic Conversion of Canola Oil to Hydrocarbons: Influence of Hybrid Catalysts and Steam. *Energy Fuels* **1995**, *9*, 599.

(32) Czernik, S.; French, R.; Feik, C.; Chornet, E. Production of Hydrogen by Catalytic Steam Reforming of "Trap Grease". To be presented at the 5th Biomass Conference of the Americas, Orlando, FL.

(33) Goering, C. E.; Schwab, A. W.; Campion, R. M.; Pryde, E. H. Fuel Properties of Eleven Vegetable Oils. *Trans. ASAE* **1982**, *25*, 1472.

(34) Bengala, D. N.; Chornet, E. Steam Reforming Catalyst and Method of Preparation. U.S. Patent 5,679,614, 1997.

(35) Medina, F.; Tichit, D.; Coq, B.; Vaccari, A.; Dung, N. T. Hydrogenation of Acetonitrile on Nickel Based Catalysts Prepared from Hydrotalcite-Like Precursors. *J. Catal.* **1997**, *167*, 142.

(36) Cavani, F.; Trifirò, F.; Vaccari, A. Hydrotalcite-Type Anionic Clays: Preparation, Properties and Applications. *Catal. Today* **1991**, *11*, 173.

(37) Velu, S.; Suzuki, K.; Okazai, M.; Kapoor, M. P.; Osaki, T.; Ohashi, F. Oxidative Steam Reforming of Methanol over CuZnAl(Zr)-oxide Catalysts for the Selective Production of Hydrogen for Fuel Cells: Catalyst Characterization and Performance Evaluation. *J. Catal.* **2000**, *194*, 373.

(38) Velu, S.; Suzuki, K.; Osaki, T. Oxidative Steam Reforming of Methanol over CuZnAl(Zr)-oxide Catalysts: A New and Efficient Method for the Production of CO-free Hydrogen for Fuel Cells. *Chem. Commun.* **1999**, *23*, 2341.

(39) Perego, C.; Peratello, S. Experimental Methods in Catalytic Kinetics. *Catalysis Today* **1999**, *52*, 133.

(40) Satterfield, C. N. *Heterogeneous Catalysis in Industrial Practice*, 2nd ed.; McGraw-Hill: New York, 1991

(41) Ridler, D. E.; Twigg, M. V. Steam Reforming. In *Catalyst Handbook*; Twigg, M. V., Ed.; Wolfe Publishing Ltd: Cleveland, U.K., 1989; Chapter 5.

(42) Leysen, R. Perspectivas Globales de Utilización de Grasas y Aceties. Presente y Futuro. *Grasas Aceites (Sevilla)* **1996**, *47*, 335.

Received for review February 12, 2001
Revised manuscript received July 9, 2001
Accepted July 27, 2001

IE010135T